Ecological impact due to the implementation of a modeled and optimized hybrid system

Othmane Echarradi[1], Abdessamad Benlafkih[2], Abdelkader Hadjoudja[3], Mounir Fahoume[1]
[1]Laboratory of Material Physics and Subatomic, Faculty of Sciences, Ibn-Tofail University, Kenitra, Morocco
[2]Advanced Systems Engineering Laboratory, National School of Applied Sciences, Ibn-Tofail University, Kenitra, Morocco
[3]Laboratory of Electronic Systems, Information Processing, Mechanics and Energetics, Faculty of Sciences, Ibn-Tofail University, Kenitra, Morocco

Article Info	ABSTRACT

This paper presents a very alarming forecasts about our future and particularly for a medium and long-term future. That is to say, several actions are being carried out by different civil and state parties to deal with these very concrete threats. And it is within this framework that this paper fits, and its objective is to highlight the hybrid systems and more precisely the photovoltaic-wind hybrid systems coupled with storage batteries, as an efficient alternative to the classical means of electricity production. This work will adopt a method of obtaining results called performance evaluation, so this manuscript will present firstly the mathematical model of this hybrid system to best conceive what it is about, then as second part will determine the exact figures of the largest amount of carbon dioxide (CO_2) that can be avoided using this technology and following a precise methodology, this can be applied to our situation, i.e., a simple house or to any other type of installation.

This is an open access article under the CC BY-SA license.

Corresponding Author:

Othmane Echarradi
Laboratory of Material Physics and Subatomic, Faculty of Sciences, Ibn-Tofail University
BP 242, 14000 Kenitra, Morocco
Email: echarradi.othmane@gmail.com

1. INTRODUCTION

The use of fossil fuels is becoming a real threat to life on planet earth, indeed the repeated natural disasters and droughts in countries hitherto spared, testify to the seriousness of the situation [1]. Other factors such as the scarcity of these same sources, which are now essential for our survival, push us to look for new alternatives or to improve existing technology [2], [3]. The renewable energies such as solar or wind power remain the preferred path towards a radical solution to these problems.

Hybrid systems [4] can have a say in this situation if conditions are met. Especially good wind, solar resource and more importantly a willingness on the part of individuals to adopt this type of technology. Indeed, the photovoltaic (PV)-wind hybrid technology which combines wind energy and solar energy is forced to guarantee with a fairly high probability an availability of electricity throughout the day and over the seasons, since these two forms of energy are very complementary.

This paper can be considered as a contribution to the work already carried out by millions of people who want things to change quickly, so during this work the functioning of this hybrid wind-PV system with battery storage will be dissected, as well as all the elements constituting this same system and that by modeling them one by one with mathematical models. Then a whole section will be dedicated to optimizing the sizing of the installation [5] following one of the six existing methods, namely: the graphic construction method, the probabilistic method, the analytical method, the iterative method, the artificial intelligence (AI)

method and the hybrid method, however the solution chosen to optimize our hybrid system is one of the analytical methods and more precisely the hybrid optimization of multiple electric renewables (HOMER) software given its formidable efficiency. Then comes as a downstream work the procedure of the determination of the exact maximum amount of carbon dioxide (CO_2) that this system allows to avoid [6] during the life of the project. Thus, giving an idea of the importance that this type of system can play for the well-being of the environment, even on a small scale here a domestic installation.

2.   METHOD

In this section the hybrid system in question will be briefly modeled and then optimized [7] according to an analytical method. This allows the extraction of the combination that will be manipulated to achieve the desired goal. And here, our main objective is to determine the greatest amount of CO_2 that can be avoided using this device.

2.1. Modeling of the hybrid system under study

As mentioned before, the interest is focused in the wind-PV hybrid system and more precisely, the one with battery storage [8], [9] and with a connection to the public distribution networks. All its elements will be dissected later. This system [10] is illustrated in Figure 1.
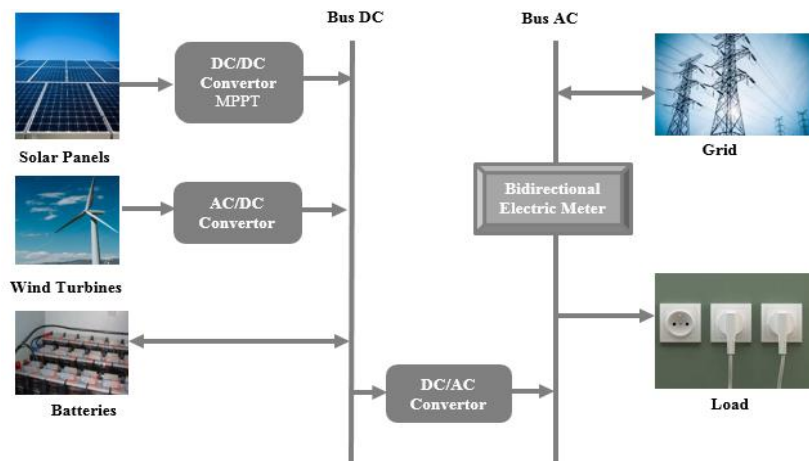

Figure 1. Synoptic of the system studied

2.1.1. Modeling of the photovoltaic assembly

The next step is to model the photovoltaic system. The device in question is illustrated in the Figure 2. The system is composed of three main elements, PV generator [11], chopper and the control system.

a. Modeling of the photovoltaic cell

Typically, a photovoltaic cell [12] can be presented as shown in the Figure 3. This cell is composed of a current source, a diode and resistors. Figure 3 illustrates a modeled photovoltaic cell.
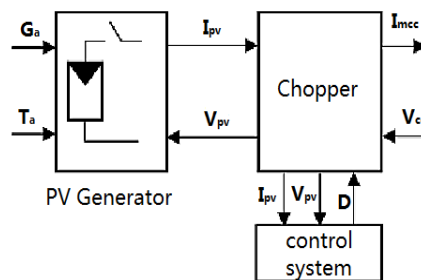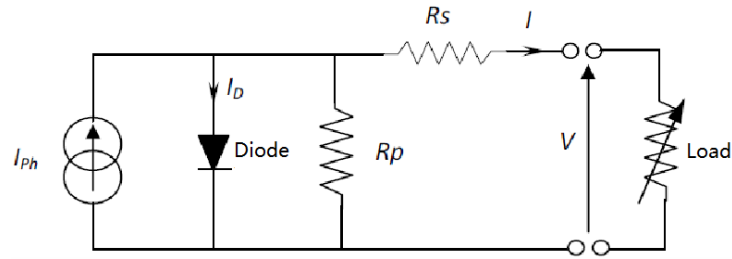

Figure 2. Photovoltaic system studied

Figure 3. Single diode model of a PV cell

After calculations and simplifications, the current of the cell can be given in the following form:

$$I = I_{ph} - I_{sat}\left(\exp\left(\frac{q.(V+I.R_S)}{n.k.T_C}\right) - 1\right) - \frac{V+I.R_S}{R_P}$$

or again, knowing that the value of R_p is large enough:

$$I = I_{ph} \times \left[1 - \frac{\left(\exp\left(\frac{V+I.R_S}{n.V_T}\right) - 1\right)}{\left(\exp\left(\frac{V_{co}}{n.V_T}\right) - 1\right)}\right]$$

where I_{sat} is the diode saturation current or dark current, n ideality coefficient of the photovoltaic cell, I_{ph} is the light-generated current or photocurrent, q is the electron charge, k is Boltzmann constant, T_c is the cell working temperature, V_{co} the no-load voltage, V_T the thermodynamic potential $V_T = \frac{k.T_C}{q}$.

b. Association of photovoltaic cells

In general, a photovoltaic cell cannot produce more than 2 watts. Therefore, to generate more power, a series association is made, which gives a module [13], [14], then another association or/and in parallel of several modules is made, which gives this time a photovoltaic panel as we can see on Figure 4. Two types of diodes are then added to limit the reverse voltage, one in series and one in parallel, better known as a bypass diode.
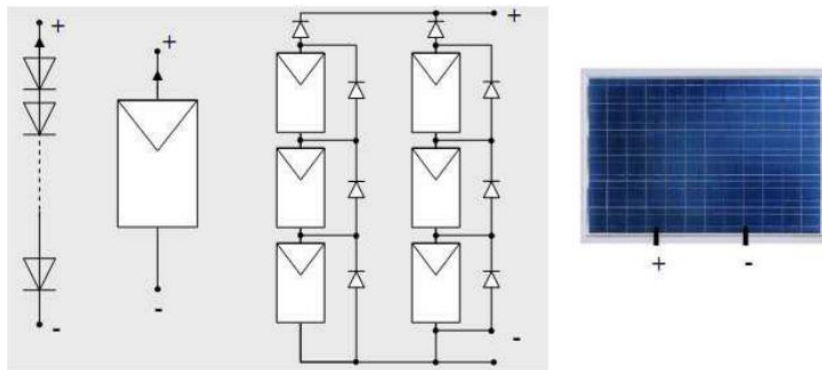

Figure 4. Composition of a photovoltaic panel

c. Modeling of the PV generator

The interest is now focused on the modeling of the photovoltaic module. This module is composed of ns cells in series and np cells in parallel. Figure 5 describes the module in question. From Figure 5, we then deduce these equations for the one-diode model:

$$I_{ph} = n_p \times i_{ph} \qquad I_G = n_p \times i_{pph} \qquad I_d = n_p \times i_d \qquad I_{rsh} = n_p \times i_{rsh}$$

$$V_d = n_s \times v_d \qquad V_G = ns \times v_p \qquad = \frac{n_s}{n_p} \times r_s \qquad R_{sh} = \frac{n_s}{n_p} \times r_p$$
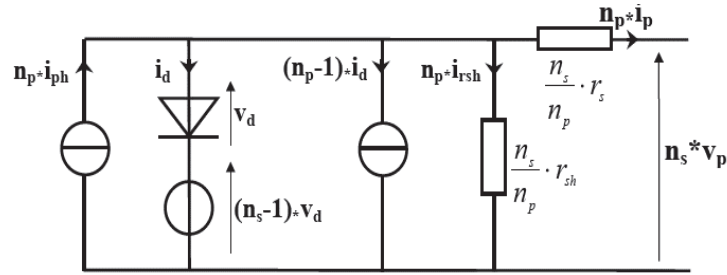
Figure 5. One-diode model of a photovoltaic module

d. Modeling of the chopper with maximum power point tracking (MPPT) control

The next step is to model the chopper with its control system [15]. It is important to know that several combinations are possible depending on the type of chopper and MPPT [16], [17] chosen. In the case of this study, the chosen configuration is a boost chopper and as a type of MPPT, an incremental inductance.

1) Boost converter modeling

As just mentioned, the chopper model chosen is a step-up chopper. It is represented in the Figure 6. This representation is a simplification obtained thanks to the mean value theorem.
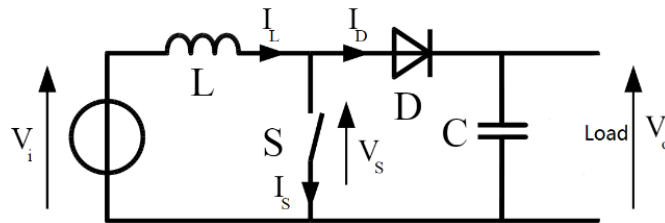

Figure 6. Diagram of a boost converter

For the boost converter three conduction modes are possible. The first is the continuous mode, the second is the discontinuous mode and finally the limit between the continuous and discontinuous conduction. The equations characterizing each mode are given in the following:

− Continuous conduction:

$$\frac{V_0}{V_i} = \frac{1}{1 - \alpha}$$

− Discontinuous conduction:

$$\frac{V_0}{V_i} = 1 + \frac{V_i \times \alpha^2 \times T}{2L \times I_0}$$

− Limit between continuous conduction and discontinuous conduction:

$$\text{Io}_{\text{lim}} = \frac{V_i \times T}{2L} \times \frac{V_i}{V_0} \times (1 - \frac{V_i}{V_0})$$

where α the duty cycle and I_0 the current flowing through the load.

2) Maximum power point tracking (MPPT) types incremental inductance

The incremental inductance algorithm is based on the fact that the MPP is reached only if dP/dV is zero. The characteristics of the photovoltaic module prove that the derivative is greater than zero on the left of the MPP and less than zero on the right of the MPP. This leads to the following set of equations:

$$\frac{dP}{dV} = 0 \text{ if } V = Vmp \quad \text{and} \quad \frac{dP}{dV} < 0 \text{ if } V > Vmp \text{ and } \frac{dP}{dV} > 0 \text{ if } V < Vmp$$

Moreover: $\frac{dP}{dV}$=I+V.$\frac{dI}{dV}$ Than: $\frac{dI}{dV} = -\frac{I}{V}$

The necessary incremental changes dV and dI are obtained by comparing the most recent measured values for V and I to those measured during the previous cycle. The central function to find the maximum power point uses the (1) and (2). This leads to the algorithm used for this method is shown in Figure 7.

$$\frac{dI}{dV} = -\frac{I}{V} \tag{1}$$

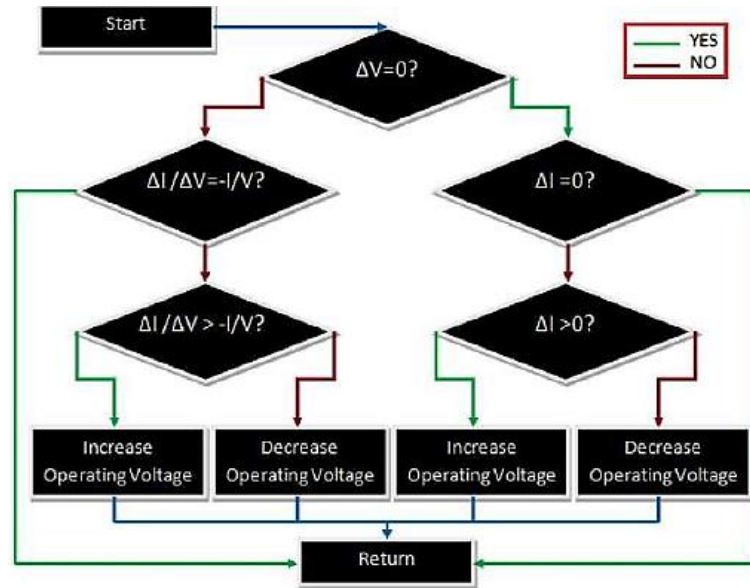$$\frac{dI}{dV} > -\frac{I}{V} \tag{2}$$

Figure 7. Conductance increment MPPT algorithm flowchart [18]

2.1.2. Modeling of the wind system
a. Wind power generated

The modeling of the wind system [19] concerns primarily the wind power generated and commonly a wind turbine on the market is characterized by its nominal power. This power is provided when there is a wind blowing at a nominal speed. The average power of the wind turbine is given by:

$$P_{eol_{moy}} = \int_0^\infty P_{eol}(v).f(v)dv$$

where $f(v)$ the probability of the speed v, $P_{eol}(v)$ the resultant power of the speed v, this latter is calculated according to the wind speed as:

$$\begin{cases} 0 & \\ P_n \frac{v^k - v_d^k}{v_n^k - v_d^k} & for \quad 0 \leq v < vd \\ & for \quad vd \leq v < v \\ P_n & for \quad vn \leq v < vc \\ 0 & for \quad vc \leq v \end{cases}$$

where P_n the nominal power of the wind turbine, v_d the turbine starting speed, v_n the rated turbine speed, v_c the turbine cut-off speed and k the form factor.

On the other hand, and after calculation, it is possible to determine a simple expression of the average power produced by the wind turbine. This power is given as the product of two terms. Its expression is presented in the following:

$$P_{avg\_power} = P_n \left[\frac{exp\left(-\left(\frac{v_d}{c}\right)^k\right) - exp\left(-\left(\frac{v_n}{c}\right)^k\right)}{\left(\frac{v_n}{c}\right)^k - \left(\frac{v_d}{c}\right)^k} - exp\left(-\left(\frac{v_c}{c}\right)^k\right) \right]$$

b. Modeling of the permanent magnet synchronous generator

   Several types of generators exist on the market but the one chosen in this study is the permanent magnet synchronous generator because of its advantages. Its model is given in the following. For an *abc* reference, the synchronous machine is represented as:

$$[V]_{(3)} = [e]_{(3)} - [R_S] \times [i]_{(3)} - [L] \times \frac{d[i]_{(3)}}{dt}$$

where:

- $[V]_{(3)} = \begin{bmatrix} V_a \\ V_b \\ V_c \end{bmatrix}$; where V_a, V_b, V_c: the instantaneous values of the voltages each phase.

- $[e]_{(3)} = P.\varnothing_f.\Omega. \begin{bmatrix} \sin(P.\Omega.t) \\ \sin\left(P.\Omega.t - \frac{2\pi}{3}\right) \\ \sin\left(P.\Omega.t - \frac{4\pi}{3}\right) \end{bmatrix}$; where P: number of generator pole pairs; $\varnothing_f$: The magnetic flux of

 magnets; Ω: generator rotation speed.

- $[R_S]_{(3)} = \begin{bmatrix} R_S & 0 & 0 \\ 0 & R_S & 0 \\ 0 & 0 & R_S \end{bmatrix}$; R_s: stator winding resistance.

- $[i]_{(3)} = \begin{bmatrix} i_a \\ i_b \\ i_c \end{bmatrix}$; where i_a, i_b, i_c: the instantaneous values of the currents at each phase.

- $[L] = \begin{bmatrix} L_S & M_{ab} & M_{ac} \\ M_{ba} & L_S & M_{bc} \\ M_{ca} & M_{cb} & L_S \end{bmatrix}$; where L_S: self-inductance of stator windings et M_{ij} mutual inductance of

 stator winding.

c. Model of the diode bridge rectifier

   The following diagram shows a rectifier fed by a three-phase voltage source. An ideal battery, as an example, supplies it. The following diagram, shown in Figure 8. The line currents i_a, i_b and i_c each take in turn the value of the direct current I_{dc}, each of the diodes ensures the conduction during 1/3 of the period. Thus, the equivalent diagram during a conduction sequence can be easily deduced. And if phase 1 and 2 are taken as an example of study, then the equivalent diagram is given as follows in the Figure 9. From the equivalent diagrams:

$$\frac{dI_{dc}}{dt} = \frac{1}{2L_S} \times (V_a - V_b - V_c)$$

2.1.3. Storage system modeling

   For this study, the interest will be focused on the CIEMAT model. This model which basic diagram is represented on the Figure 10 is characterized by only two elements, a voltage source and an internal resistance; these two values depend on several parameters. The model in question is represented on Figure 10.

   The voltage at the battery terminals is defined as a function of the imposed current, its state of charge and the temperature. It takes into account the faradic efficiency in charge to calculate the evolution of its state of charge and integrates the degassing phase. Figure 11 shows the CIEMAT model of the lead battery in Simulink.

   The inputs of the model are therefore the power and the temperature deviation from the nominal temperature set at 25 °C. The calculation of the state of charge is done internally and allows the calculation of the voltage. The value of the current is obtained thanks to the equation below, while the clock has just a role in the data acquisition. And the charging and discharging voltage are characterized by the following (3) and (4):

$$I_{bat} = \frac{P_{bat}}{V_{bat}}$$

The expression of the state of charge is given by:

$$EDC = 1 - \frac{Q_d}{C_d}$$

where C_d is the nominal capacity of the battery in (Ah), Q_d is the amount of missing charge relative to C_d.
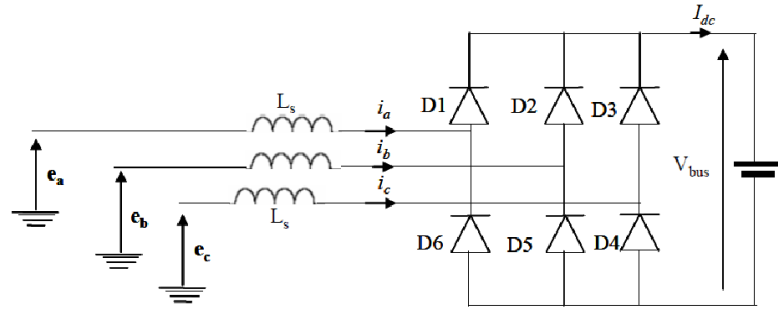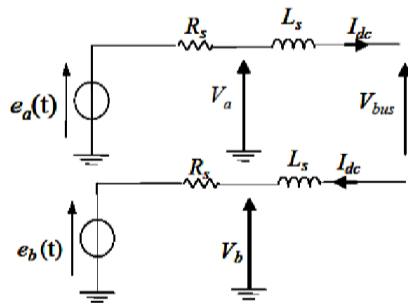

Figure 8. Diagram of a diode bridge

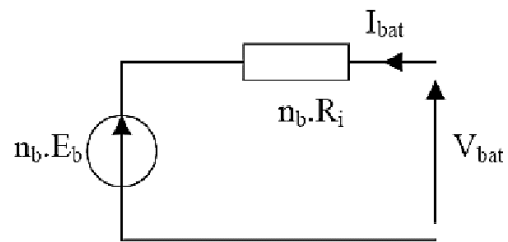Figure 9. Equivalent diagram of a normal conduction sequence
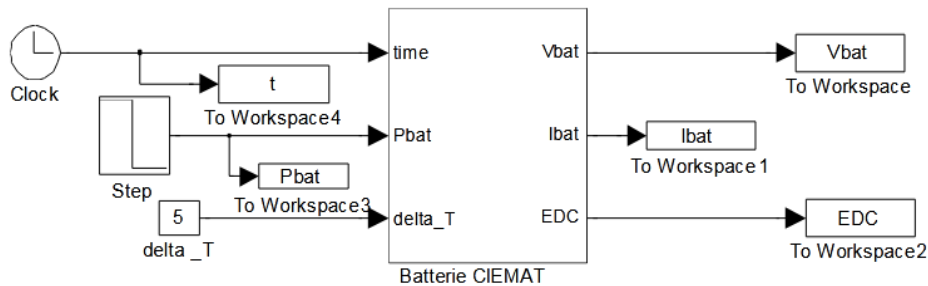
Figure 10. Equivalent diagram of n_b elements

Figure 11. CIEMAT model of the lead battery under Simulink

– Discharge voltage:

$$V_{bat_{dé}} = n_b[1.965 + 0.12 \times EDC] - n_b \frac{|I_{bat}|}{C_{10}} \times$$
$$\left(\frac{4}{1+|I_{bat}|^{1,3}} + \frac{0.27}{EDC^{1,5}} + 0.02\right) \times (1 - 0.007 \times \Delta T) \tag{3}$$

− Charging voltage:

$$V_{bat_{ch}} = n_b[2 + 0.16 \times EDC] - n_b \frac{I_{bat}}{C_{10}} \times \left(\frac{6}{1 + I_{bat}^{1,3}} + \frac{0.48}{(1 - EDC)^{1,2}} + 0.036 \right)$$
$$\times (1 - 0.025 \times \Delta T) \tag{4}$$

where the capacity C_{10} is the capacity in Ampere-hours of the battery in discharge mode at constant current for 10 hours.

2.1.4. Inverter modeling

The combination of a transistor T_i and a diode D_i gives a bidirectional component K_i. As the orders of the two transistors of the same arm are complementary, we can replace each arm of the inverter by a switch with two positions. The Figure 12 illustrates what has just been said, and the following reference provides more information on inverters [20]. For what follows, Let F_i be the state of the switch K_i, F_i is given by:

$$\begin{cases} Fi=0 & if \quad T_i \text{ is closed and } T_i' \text{ is open} \\ Fi=1 & if \quad T_i \text{ is open and } T_i' \text{ is closed} \end{cases}$$

The phase-to-phase voltages at the inverter are given by:

$$\begin{bmatrix} V_{ab} \\ V_{bc} \\ V_{ca} \end{bmatrix} = V \times \begin{bmatrix} F_1 - F_2 \\ F_2 - F_3 \\ F_3 - F_1 \end{bmatrix}$$

As a result, the phase-to-neutral voltages as well as the current at the input of the inverter are given by:

$$\begin{bmatrix} V_{sa} \\ V_{sb} \\ V_{sc} \end{bmatrix} = V \times \begin{bmatrix} 2F_1 - F_2 - F_3 \\ -F_1 + 2F_2 - F_3 \\ -F_1 - F_2 + 2F_3 \end{bmatrix} \quad And \quad I_S = F_1 I_{sa} + F_2 I_{sb} + F_3 I_{sc}.$$
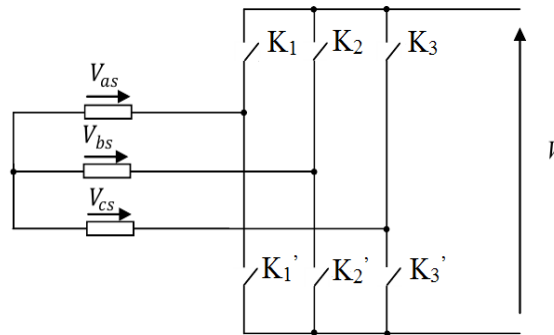

Figure 12. Representation of bidirectional components

2.2. Optimization of the sizing of the hybrid system

In this section, all the necessary values to optimize a wind-PV hybrid installation with storage batteries will be available, thanks to the meteorological data available on the National Aeronautics and Space Administration (NASA) website. We will choose here as a case study a location in the south of Morocco, namely the city of Essaouira, since this region has a large wind deposit and a good annual solar deposit as well. For the optimization [21], [22] of our installation, we will use a software solution that is no longer presented in the field of optimization of hybrid systems, it is HOMER [23].

2.2.1. Load profile

In the case of the study, i.e., for the city of Essaouira, the variations between seasons are not so important. This minimal variation between seasons allowed us to have a single consumption profile. Figure 13 shows the chosen consumption profile.
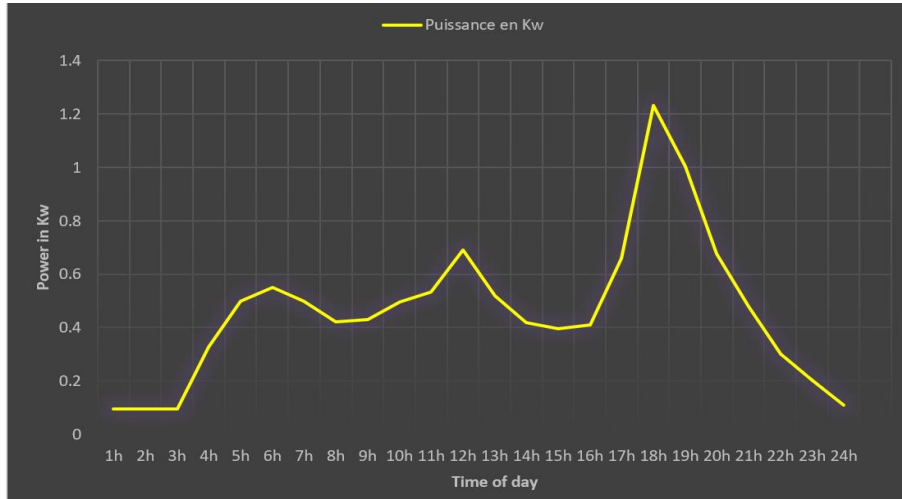
Figure 13. Electricity consumption profile chosen for our study

2.2.2. Weather data profile

a. Temperature profile

As shown in Figure 14, is the temperature profile. Table 1 gives the average daily temperature values over a year for the Essaouira region. All these values were taken from the NASA site for a period of 22 years.

Figure 14. Average daily temperature profile over a year

Table 1. Average daily temperature values over a year

Month	Average daily temperature °C
January	13,420
February	14,770
March	16,660
April	17,650
May	19,630
June	22,330
July	25,310
August	25,350
September	23,470
October	20,710
November	17,510
December	14,840

b. Wind profile

As shown in Figure 15 are the wind profile. The Table 2 on the other hand gives the average values of wind speed over the course of a year for the Essaouira region. All these values were taken from the NASA website for a period of 22 years.
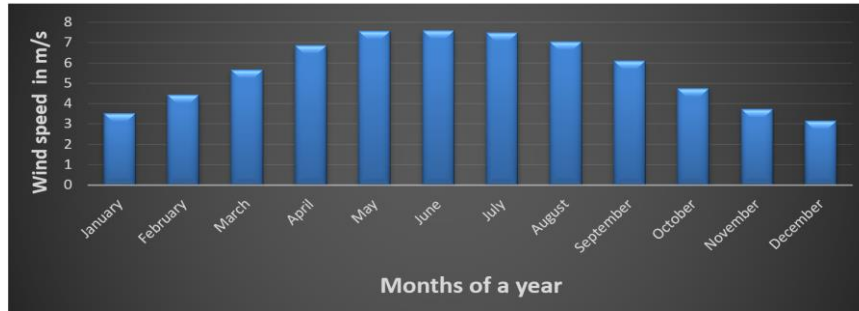
Figure 15. Average wind speed profile over a year

Table 2. Mean values of wind speed over a year

Month	Average wind speed m/s
January	5,310
February	5,530
March	6,070
April	6,610
May	6,010
June	6,160
July	6,450
August	6,210
September	5,420
October	5,030
November	5,360
December	5,410

c. Profile of solar irradiation

As shown in Figure 16 are the solar irradiation profile. The Table 3 on the other hand gives the average values of the daily temperature over the course of a year for the Essaouira region. All these values were taken from the NASA website for a period of 22 years.

Figure 16. Profile of the average daily solar irradiation and of the brightness index over the course of a year

Table 3. Average values of daily solar irradiation over a year

Month	Irradiation journalière (kWh/m²/jour)
January	3,530
February	4,440
March	5,670
April	6,880
May	7,560
June	7,610
July	7,490
August	7,050
September	6,100
October	4,740
November	3,740
December	3,150

Ecological impact due to the implementation of a modeled and optimized hybrid … (Othmane Echarradi)

2.2.3. Characteristics of the selected system

The characteristics of the hybrid system have been carefully chosen. Indeed, this choice was based on the demand of the domestic installation in electricity but also on the quality of these components. The elements constituting this hybrid system are given in the following.

a. Photovoltaic panels: for this component our choice fell on the American brand SunPower and more specifically for its X21-355-BLK solar panel, with a nominal power of 355 W, an efficiency of 21%, composed of 96 cells, monocrystalline, with a lifespan of 25 years and which costs 145 USD.

b. Wind turbine: for this part we chose the AWS-HC1.8 Kw wind turbine of Australian origin which has a nominal power of 1,800 W, a rated wind speed of 10.5 m/s, a lifespan of 20 years and which costs 4,950 USD.

c. Storage system: for the batteries, we chose the American brand Trojan battery, lead-acid battery, with a nominal voltage of 12 V, a capacity of 257 Ah and which costs 425 USD.

d. Inverter: for the inverter we chose the Fronius Symo 4.5-3-S of the same brand, with a capacity of 4.5 Kw and which costs 1,244 USD.

2.2.4. Conditions considered and imposed for our case study

To clarify the perspectives of this project, some assumptions are imposed, more exactly two assumptions. The first one concerns the selling price of electricity while the second one concerns the life span of the project. These conditions are given in the following:

a. The sale of electricity is permitted for the price of 0.08 USD. The main reason is the fact that the sale of electrical energy is still not allowed in Morocco but the sale of electricity by individuals is probably the future of energies.

b. The project has a lifespan of 20 years. Since it is an average duration of such a project.

2.2.5. Analysis of the results of the optimization of the hybrid system by HOMER

After calculation, HOMER presents 8 optimal solutions as shown in Figure 17. The best solution from an economic point of view remains the one involving only the public grid and solar panels as shown in the Figure 17. However, our main objective is to reduce the amount of CO_2 emitted as much as possible, so we choose the 4th solution since it has the highest installed green power by far.

Architecture										Cost				System	
⚠			SPR-X21 (kW)	AWS1.8kW	SSIG 12 255	Grid (kW)	Fron4.5 (kW)	Dispatch	COE ($)	NPC ($)	Operating cost ($/yr)	Initial capital ($)	Ren Frac (%)	Total Fuel (L/yr)
		12.0			999 999	9.87	CC	-0,0273 €	-7 758 €	-1 359 €	7 976 €	92.1	0
		12.0		2	999 999	9.87	CC	-0,0248 €	-7 042 €	-1 370 €	8 824 €	92.1	0
		12.0	1		999 999	10.5	CC	-0,0191 €	-5 988 €	-1 649 €	13 112 €	96.1	0
		12.0	1	2	999 999	10.2	CC	-0,0169 €	-5 257 €	-1 651 €	13 859 €	96.1	0
					999 999		CC	0.120 €	5 710 €	493.09 €	0,00 €	0	0
				2	999 999	0.0268	CC	0.135 €	6 434 €	481.51 €	857.56 €	0	0
			1		999 999	0.167	CC	0.197 €	9 478 €	386.95 €	4 997 €	25.7	0
			2	2	999 999	0.271	CC	0.292 €	14 451 €	312.99 €	10 826 €	41.9	0

Figure 17. Optimal solutions proposed by HOMER

The chosen solution requires a capital of 13,858.70 USD, 4,950 USD for a wind turbine type AWS-HC1.8 Kw, 5,193.96 USD for the purchase of 12 solar panels of type X21-355-BLK, 2,864.74 USD for the Fronius Symo 4.5-3-S type inverter and finally two Trojan SSIG 12 255 batteries for the price of 850 USD. From an energetic point of view the Table 4 summarizes the amount of energy produced by each element of the hybrid system, while in the Table 5 are presented the amount of energy consumed:

Table 4. Quantity of energy produced by each element during a year

Elements	kWh/year	%
X21-355-BLK	23,423	83.6
AWS-HC1.8Kw	3,535	12.6
Public network purchases	1,050	3.75
Total	28,007	100

Table 5. Quantity of energy produced by each element during a year

Elements	kWh/year	%
AC primary loads	4,109	15.3
DC primary loads	0	0
Sales to the public network	22,814	84.7
Total	26,923	100

3. RESULTS AND DISCUSSION

The main objective is to be able to reduce the CO_2 emissions of the domestic installation, which in normal times is supplied by the public distribution network, however a first result this time of an economic nature emerges [24]. This result could play its role in the adoption of this kind of technology. The two economic and environmental parts will be dealt with in what follows.

3.1. The economic result

In addition to its objective for environmental purposes, this project also aims to be financially lucrative. The financial aspect is important as it can be a source of additional motivation. As a matter of fact, this project would be able to generate no less than 33690 USD over its lifespan. The cash flow is shown in Figure 18.
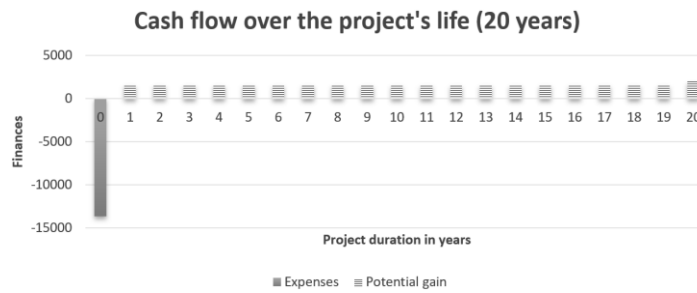

Figure 18. Cash flow for the chosen solution

3.2. Study of the carbon footprint of the chosen solution

The study is now at the stage of obtaining the results concerning greenhouse gases. Thus, the focus will be on calculating the carbon footprint of the HOMER optimized system. Table 6 contains important details for acquiring important results. To be able to determine the carbon footprint of this system, it is first necessary to determine the carbon footprint of the energy purchased from the Moroccan public network. The percentages differ from one source to another as can be seen in Table 7. The Table 7 is dedicated to this subject. Thus, the carbon footprint of one kilowatt-hour of electricity produced in Morocco is 623.58 g/kWh. Therefore, the determination of the carbon footprint of the hybrid installation is now possible. Table 8 gives all the details of this calculation. And from the table we can deduce the amount of carbon emissions avoided over one year and which is at least: 15,73 tons of CO_2/year. This result may seem enormous, but unfortunately, it is indeed the case, since for comparison purposes it represents no less than 116,500 km covered by car with combustion engine, which is really a big number. Which means, if this kind of hybrid system [25] is used massively, the quantity of CO_2 avoided will be consequently more important and will slow down the damage caused by these toxic gases while waiting for more interesting initiatives from the governments.

Table 6. Quantity of CO_2 emissions for each energy source

Elements	kWh/year	Carbon footprint over one year in kg	Carbon footprint over the life of the project in kg
X21-355-BLK	23,423	1,028.27	20,565.4
AWS-HC 1.8 kW	3,535	44.89	897.8
Public network purchases	1,050	654.76	13,095.2
Total	28,007	1,727.92	34,558.4

Table 7. CO_2 contribution of each energy source for one kWh in Morocco

Sources of energy	CO_2 emissions per kWh	Sources
Onshore wind turbine	12.7 g	ADEME
Offshore wind turbine	14.8 g	ADEME
Fossil gas	490 g	GIEC
Coal	820 g	GIEC
Photovoltaic solar	43.9 g	ADEME
Oil	510 g	ADEME
Hydraulic	43 g	GIEC
Concentrating Solar	22 g	GIEC

Table 8. Quantity of CO_2 emitted by the hybrid system

Sources of energy	Contribution in the production	Emission contribution in one kWh produced
Coal	67.6%	554.32
Oil	1.5%	7.65
Onshore wind turbine	11.6%	1.47
Fossil gas	11.8%	57.82
Hydraulic	3.2%	1.37
Concentrating Solar	4.3%	0.946

4. CONCLUSION

From the latest results of this study, one thing is certain: the transition to renewable energy is the right way to go, and this because, as the figures show, it does many good to our environment. The use of hybrid systems could be the cause of an important movement led by friends of the environment. And if the weather situation, financial conditions and enough space to accommodate this kind of equipment are met, this change could come on the one hand from everyone and on the other hand from state agencies. However, the best solution remains that these two parties help each other to promote the use of this kind of system, which can even serve from another point of view as financial project. Also promoting the sale of energy at attractive prices, particularly in developing countries that could be an important detail to consider.

REFERENCES

[1]   M. M. Samy, R. E. Almamlook, H. I. Elkholy, and S. Barakat, "Decision-making and optimal design of green energy system based on statistical methods and artificial neural network approaches," *Sustainable Cities and Society*, vol. 84, Sep. 2022, doi: 10.1016/j.scs.2022.104015.
[2]   M. M. Samy, M. I. Mosaad, M. F. El-Naggar, and S. Barakat, "Reliability support of undependable grid using green energy systems: economic study," *IEEE Access*, vol. 9, pp. 14528–14539, 2021, doi: 10.1109/ACCESS.2020.3048487.
[3]   M. M. Samy, M. I. Mosaad, and S. Barakat, "Optimal economic study of hybrid PV-wind-fuel cell system integrated to unreliable electric utility using hybrid search optimization technique," *International Journal of Hydrogen Energy*, vol. 46, no. 20, pp. 11217–11231, Mar. 2021, doi: 10.1016/j.ijhydene.2020.07.258.
[4]   M. Garip, E. Sulukan, and M. S. Celiktas, "Optimization of a grid-connected hybrid energy system: Techno-economic and environmental assessment," *Cleaner Energy Systems*, vol. 3, Dec. 2022, doi: 10.1016/j.cles.2022.100042.
[5]   M. M. Samy, H. I. Elkholy, and S. Barakat, "Multi-objective optimization of hybrid renewable energy system based on biomass and fuel cells," *International Journal of Energy Research*, vol. 45, no. 6, pp. 8214–8230, 2021, doi: 10.1002/er.5815.
[6]   S. Barakat, A. Emam, and M. M. Samy, "Investigating grid-connected green power systems' energy storage solutions in the event of frequent blackouts," *Energy Reports*, vol. 8, pp. 5177–5191, Nov. 2022, doi: 10.1016/j.egyr.2022.03.201.
[7]   M. B. Eteiba, S. Barakat, M. M. Samy, and W. I. Wahba, "Optimization of an off-grid PV/Biomass hybrid system with different battery technologies," *Sustainable Cities and Society*, vol. 40, pp. 713–727, Jul. 2018, doi: 10.1016/j.scs.2018.01.012.
[8]   J. Khalfi, N. Boumaaz, A. Soulmani, and E. M. Laadissi, "An electric circuit model for a lithium-ion battery cell based on automotive drive cycles measurements," *International Journal of Electrical and Computer Engineering (IJECE)*, vol. 11, no. 4, pp. 2798–2810, Aug. 2021, doi: 10.11591/ijece.v11i4.pp2798-2810.
[9]   S. R. Salkuti, "Electrochemical batteries for smart grid applications," *International Journal of Electrical and Computer Engineering (IJECE)*, vol. 11, no. 3, pp. 1849–1856, Jun. 2021, doi: 10.11591/ijece.v11i3.pp1849-1856.
[10]   A. O. Ogunde *et al.*, "The design of a hybrid model-based journal recommendation system," *Advances in Science, Technology and Engineering Systems Journal*, vol. 5, no. 6, pp. 1153–1162, 2020, doi: 10.25046/aj0506139.
[11]   S. Jenkal *et al.*, "Development of a photovoltaic characteristics generator based on mathematical models for four PV panel technologies," *International Journal of Electrical and Computer Engineering (IJECE)*, vol. 10, no. 6, pp. 6101–6110, Dec. 2020, doi: 10.11591/ijece.v10i6.pp6101-6110.
[12]   F. Zhang, C. Han, M. Wu, X. Hou, X. Wang, and B. Li, "Global sensitivity analysis of photovoltaic cell parameters based on credibility variance," *Energy Reports*, vol. 8, pp. 7582–7588, Nov. 2022, doi: 10.1016/j.egyr.2022.05.280.
[13]   A. Barbón, M. Ghodbane, L. Bayón, and Z. Said, "A general algorithm for the optimization of photovoltaic modules layout on irregular rooftop shapes," *Journal of Cleaner Production*, vol. 365, Sep. 2022, doi: 10.1016/j.jclepro.2022.132774.
[14]   D. Peng, Z. Fang, X. Yu, and Q. Huang, "Characteristic analysis of patterned photovoltaic modules for building integration," *Energy Conversion and Management*, vol. 276, Jan. 2023, doi: 10.1016/j.enconman.2022.116524.
[15]   M. O. Rachedi, M. L. Saidi, and F. Arbaoui, "MPPT control design for variable speed wind turbine," *International Journal of Electrical and Computer Engineering (IJECE)*, vol. 10, no. 5, pp. 4604–4614, 2020, doi: 10.11591/ijece.v10i5.pp4604-4614.
[16]   S. Manna *et al.*, "Design and implementation of a new adaptive MPPT controller for solar PV systems," *Energy Reports*, vol. 9, pp. 1818–1829, Dec. 2023, doi: 10.1016/j.egyr.2022.12.152.
[17]   B. Patra, P. Nema, M. Z. Khan, and O. Khan, "Optimization of solar energy using MPPT techniques and industry 4.0 modelling," *Sustainable Operations and Computers*, vol. 4, pp. 22–28, 2023, doi: 10.1016/j.susoc.2022.10.001.
[18]   A. Benlafkih and M. Chafik Elidrissi, "Boost converter system modelling and incremental conductance algorithm for photovoltaic system via Matlab/Simulink," *Proceedings of the Third International Conference on Computing and Wireless Communication Systems, ICCWCS 2019, April 24-25, 2019, Faculty of Sciences, Ibn Tofaïl University-Kénitra-Morocco*, 2019, doi: 10.4108/eai.24-4-2019.2284106.
[19]   A. A. Kadhem, N. I. A. Wahab, and A. Abdalla, "The contribution of wind energy capacity on generation systems adequacy reliability using differential evolution optimization algorithm," *Advances in Science, Technology and Engineering Systems Journal*, vol. 5, no. 6, pp. 331–340, 2020, doi: 10.25046/aj050640.
[20]   K. Dhineshkumar, C. Subramani, A. Geetha, and C. Vimala, "Performance analysis of PV powered multilevel inverter," *International Journal of Electrical and Computer Engineering (IJECE)*, vol. 9, no. 2, pp. 753–760, Apr. 2019, doi: 10.11591/ijece.v9i2.pp753-760.

[21] M. Thirunavukkarasu, Y. Sawle, and H. Lala, "A comprehensive review on optimization of hybrid renewable energy systems using various optimization techniques," *Renewable and Sustainable Energy Reviews*, vol. 176, Apr. 2023, doi: 10.1016/j.rser.2023.113192.

[22] A. F. Güven, N. Yörükeren, and M. M. Samy, "Design optimization of a stand-alone green energy system of university campus based on Jaya-Harmony search and ant colony optimization algorithms approaches," *Energy*, vol. 253, Aug. 2022, doi: 10.1016/j.energy.2022.124089.

[23] Muskan and H. Kaur Channi, "Optimal designing of PV-diesel generator-based system using HOMER software," *Materials Today: Proceedings*, Jan. 2023, doi: 10.1016/j.matpr.2023.01.053.

[24] A. F. Tazay, M. M. Samy, and S. Barakat, "A techno-economic feasibility analysis of an autonomous hybrid renewable energy sources for University building at Saudi Arabia," *Journal of Electrical Engineering and Technology*, vol. 15, no. 6, pp. 2519–2527, Nov. 2020, doi: 10.1007/s42835-020-00539-x.

[25] M. M. Samy, H. H. Sarhan, S. Barakat, and S. A. Al-Ghamdi, "A hybrid PV-biomass generation based micro-grid for the irrigation system of a major land reclamation project in Kingdom of Saudi Arabia (KSA)-case study of Albaha area," in *2018 IEEE International Conference on Environment and Electrical Engineering and 2018 IEEE Industrial and Commercial Power Systems Europe (EEEIC / I&CPS Europe)*, Jun. 2018, pp. 1–8, doi: 10.1109/EEEIC.2018.8494543.

BIOGRAPHIES OF AUTHORS

Othmane Echarradi 🆔 ⚄ sc ↻ graduated from the "Mohammadia School of Engineer" known as EMI, he has during his professional career ensured several positions of responsibility, notably in companies such as BATRAF and SI3, both located in his hometown Marrakech, he occupies at present the position of general manager of the Elec and Beyond design office, also and since 2021 he is a Ph.D. candidate at Ibn Tofail University in Kenitra in Morocco. He can be contacted at email: echarradi.othmane@gmail.com.

Abdessamad Benlafkih 🆔 ⚄ sc ↻ received the B.S. and M.S. degrees, from university of sciences Dhar El Mehraz Fez, In 1997 and 2003, Respectively. And the Ph.D. degree in electrical engineering from university ibn Tofail Kenitra in 2015. He was a teacher in secondary cycle from 2004 to 2020. And in 2020, he has been a professor of electrical power engineering in University Ibn Tofail Kenitra Morocco. He can be contacted at email: abdessamad.benlafkih@uit.ac.ma.

Abdelkader Hadjoudja 🆔 ⚄ sc ↻ was an engineer and was awarded a doctorate in Microelectronic by the National Polytechnic Institute of Grenoble, France, in 1997. He worked for 6 years as PLD Leader Engineer Software in Atmel, Grenoble, France, and as a Consultant within Design and Reuse. Since July 2010, he became a full Professor of Electronics in Ibn Tofail University Kenitra. He can be contacted at email: abdelkader.hadjoudja@uit.ac.ma.

Mounir Fahoume 🆔 ⚄ sc ↻ obtained his doctorate in 2002 at the Mohammed V University of Rabat-Morocco. He is a professor of physics at the Faculty of Sciences of Kenitra at Ibn Tofail-Morocco University. His research interests include renewable energies, the elaboration and characterization of thin-film semiconductors for photovoltaic applications. He can be contacted at e-mail: mounir.fahoume@uit.ac.ma.